metals

MDPI

Review

Research Progress in Corrosion Behavior and Anti-Corrosion Methods of Steel Rebar in Concrete

Qiuyue Wang [1,2], Zilong Wang [1], Chengtao Li [3], Xinglong Qiao [1], Hao Guan [1], Zhou Zhou [1,*] and Dan Song [1,*]

[1] College of Materials Science and Engineering, Hohai University, Nanjing 211100, China; wangqiuyue@jmi.edu.cn (Q.W.); 2117020308@hhu.edu.cn (Z.W.); 221608010037@hhu.edu.cn (X.Q.); 211608010014@hhu.edu.cn (H.G.)
[2] School of Naval Architecture & Intelligent Manufacturing, Jiangsu Maritime Institute, Nanjing 211170, China
[3] Suzhou Nuclear Power Research Institute Co., Ltd., Suzhou 215004, China; lichengtao@cgnpc.com.cn
* Correspondence: specific_z@hhu.edu.cn (Z.Z.); songdancharls@hhu.edu.cn (D.S.)

Abstract: The corrosion of steel rebars is a prevalent factor leading to the diminished durability of reinforced concrete structures, posing a significant challenge to the safety of structural engineering. To tackle this issue, extensive research has been conducted, yielding a variety of theoretical insights and remedial measures. This review paper offers an exhaustive analysis of the passivation processes and corrosion mechanisms affecting steel rebars in reinforced concrete. It identifies key factors such as chloride ion penetration and concrete carbonization that primarily influence rebar corrosion. Furthermore, this paper discusses a suite of strategies designed to enhance the longevity of reinforced concrete structures. These include improving the concrete protective layer's quality and bolstering the rebars' corrosion resistance. As corrosion testing is essential for evaluating steel rebars' resistance, this paper also details natural and accelerated corrosion testing methods applicable to rebars in concrete environments. Additionally, this paper deeply presents an exploration of the use of X-ray computed tomography (X-CT) technology for analyzing the corrosion byproducts and the interface characteristics of steel bars. Recognizing the close relationship between steel bar corrosion research and microstructural properties, this paper highlights the pivotal role of X-CT in advancing this field of study. In conclusion, this paper synthesizes the current state of knowledge and provides a prospective outlook on future research directions on the corrosion of steel rebars within reinforced concrete structures.

Keywords: reinforced concrete; corrosion of rebar; X-CT technology; investigation methods

Citation: Wang, Q.; Wang, Z.; Li, C.; Qiao, X.; Guan, H.; Zhou, Z.; Song, D. Research Progress in Corrosion Behavior and Anti-Corrosion Methods of Steel Rebar in Concrete. *Metals* **2024**, *14*, 862. https://doi.org/10.3390/met14080862

Academic Editors: Mosab Kaseem and Petros E. Tsakiridis

Received: 28 June 2024
Revised: 16 July 2024
Accepted: 24 July 2024
Published: 26 July 2024

1. Introduction

Reinforced concrete structures have the advantages of low cost, simple construction, and convenient material acquisition, making them widely used in construction engineering [1]. Despite the emergence of new building materials and structural forms, concrete structures still hold an irreplaceable position in construction engineering such as concrete frame structures for residential, industrial, and other types of buildings including high-rises, bridges, and airport terminals. However, the durability of a material or a structure is a critical factor. The lifespan of materials should be prolonged for two reasons: one economic and the other being sustainable motivations and preventing premature failure.

The durability of concrete structures is affected by various factors, particularly steel corrosion and aggregate reaction stress, weathering, freeze–thaw cycling, etc. Of these, the corrosion of steel rebars can result in cracks or even detachment in concrete, significantly diminishing the service life of concrete structures [2–6]. Within the marine climate, chloride and other corrosive agents persistently assault the concrete structure, leading to its gradual degradation. This relentless erosion accelerates the corrosion process of steel reinforcement bars. Consequently, this ultimately results in the deterioration of the durability of reinforced concrete structures, compromising their structural integrity. This poses a significant

challenge to the safe and sustained operation, as well as the longevity, of reinforced concrete structural engineering projects [7,8].

To effectively address this challenge, it is imperative to conduct a thorough investigation into the corrosion behavior and corrosion control techniques pertaining to steel bars embedded within concrete [9–12]. In a previous review, we focused on summarizing the macrocell corrosion mechanism of steel bars in concrete [1]. Presently, a diverse array of technological approaches has been developed to tackle the issue of steel corrosion and thereby extend the service life of reinforced concrete structures. Amongst these techniques, a fundamental approach to enhancing the durability of reinforced concrete involves the augmentation of the corrosion resistance properties inherent to the steel rebars themselves. In response to this need, stainless steel reinforcement [13,14], coated reinforcement [15,16], and alloy corrosion-resistant reinforcement [17,18] have emerged as viable solutions. Depending on their inherent strengths and weaknesses, these steel rebars can be selectively employed in construction projects tailored to specific usage environments and service lifetimes. The primary advantage of alloyed steel rebars lies in their capacity to fine-tune their microstructure through the meticulous design of alloy element types and concentrations, thus attaining strength and toughness that adhere to established standards [19–22]. Alloying significantly bolsters the corrosion resistance of steel rebars, while simultaneously maintaining cost-effective production processes. In this paper, a comprehensive overview of the diverse passivation and corrosion mechanisms pertaining to steel rebars within reinforced concrete structures is presented. Furthermore, the pivotal factors that govern the corrosion of steel rebars within concrete, such as chloride ion ingress and concrete carbonation, are comprehensively investigated. A diverse array of methodologies aimed at enhancing the durability of reinforced concrete structures is also introduced, particularly summarizing the research progress on corrosion-resistant alloy steel rebars. This paper serves as a valuable resource for researchers delving into the corrosion mechanisms of steel rebars within concrete structures. Enhancing the durability and prolonging the service lifespan of reinforced concrete structures holds paramount significance.

2. Passivation and Corrosion Mechanisms of Steel Rebars in Concrete

2.1. Passivation of Steel Rebars in Concrete

The mechanism for the formation of the steel rebar passivation film mainly concerns the influence of the alkaline environment within the concrete on the surface of the rebar. Ordinary Portland cement is a key raw material in concrete preparation, characterized by a high concentration of calcium salts. Following the hydration reaction, a significant quantity of alkaline substances like calcium hydroxide is generated, leading to a substantial elevation in the alkalinity of the pore fluid in concrete (typically with a pH value around 12.5) [23–26]. The reaction for forming the passivation film on conventional carbon steel bars is as outlined below:

$$8\left(OH^-\right) + 3Fe \rightarrow Fe_3O_4 + 4H_2O + 8e^- \quad (1)$$

$$6\left(OH^-\right) + 2Fe \rightarrow Fe_2O_3 + 3H_2O + 6e^- \quad (2)$$

$$3\left(OH^-\right) + Fe \rightarrow FeOOH + H_2O + 3e^- \quad (3)$$

The aforementioned reaction equations demonstrate that the high alkalinity of the concrete pore fluid is essential for the formation of a passivation film on steel rebars and for creating an environment that preserves the film's stability. This alkaline environment is crucial for preventing corrosion. However, the exposure of concrete structures to aggressive environments, such as marine, saline lake, and saline–alkali soil conditions, introduces external corrosive agents that infiltrate the concrete's interior. This infiltration leads to a dilution of the pore fluid's alkaline concentration, compromising the protective capacity of the passivation film. Concurrently, chloride ions, in particular, persistently attack the steel reinforcement matrix. Their presence initiates the breakdown of the passivation film, which is instrumental in shielding the steel from corrosion. The continuous erosion by

chloride ions eventually results in the degradation of this protective layer, leaving the steel reinforcement susceptible to corrosion.

2.2. Corrosion Process of Steel Rebars in Concrete

To enhance the durability of reinforced concrete structures, it is imperative to delve deeply into the corrosion mechanisms of the steel reinforcements embedded within the concrete matrix. The predominant electrochemical mechanism of reinforcement corrosion can be delineated as follows [27,28]: Subsequent to the disintegration of the passivation layer, the reinforcement matrix is subjected to an anodic oxidation reaction (4), entailing electron forfeiture by the anode and its subsequent transmutation into Fe^{2+}. Electrons traverse to the cathode via the concrete's pore fluid, engaging in a reduction reaction (5) with the O_2 proximal to the steel reinforcement, culminating in the prolific generation of (OH^-). During the cathodic reaction phase, hydroxyl ions (OH^-) interact with ferrous ions (Fe^{2+}) (6) to facilitate the formation of iron(II) hydroxide ($Fe(OH)_2$). In the presence of oxygen (O_2) and water, the steel reinforcements continuously undergo corrosion reactions (7) (8), ultimately resulting in the formation of red rust, specifically iron (III) oxide (Fe_2O_3), on the surface of the concrete matrix.

Due to the numerous pores present at the interface between steel bars and concrete, rust continues to accumulate at this interface following the corrosion of the steel bars [29]. As the thickness of the rust layer gradually increases, the expansion force exerted by the rust at the steel–concrete interface is induced, leading to the development of rust expansion cracks within the concrete matrix. The propagation of these cracks is influenced by the mechanical properties of the concrete, the bond strength between the steel and the concrete, and the local environmental conditions. Eventually, the rust expansion cracks gradually propagate towards the surface of the concrete, ultimately resulting in the formation of through cracks, as illustrated in Figure 1. At this stage, the corrosion process persists, as the existence of penetrating cracks facilitates the accelerated diffusion of substances, including chloride ions (Cl^-), towards the steel matrix surface, thus intensifying the corrosion process [30]. Chloride ions not only accumulate in the pitting areas during the corrosion process but also accumulate in the surrounding areas, which further accelerates the corrosion process. As the corrosion process continues unabated, the structural integrity of the reinforced concrete is progressively compromised. The expansion and cracking can lead to spalling of the concrete cover, loss of bond between the steel and the concrete, and a reduction in the load-carrying capacity of the rebars. Over time, this can result in a significant reduction in the service life of the reinforced concrete structures and may necessitate costly repairs or replacements.

$$Fe \rightarrow Fe^{2+} + 2e^- \tag{4}$$

$$O_2 + 2H_2O + 4e^- \rightarrow 4\left(OH^-\right) \tag{5}$$

$$2\left(OH^-\right) + Fe^{2+} \rightarrow Fe(HO)_2 \tag{6}$$

$$4Fe(HO)_2 + O_2 + 2H_2O \rightarrow 4Fe(HO)_3 \downarrow \tag{7}$$

$$2Fe(HO)_3 \rightarrow Fe_2O_3 \cdot H_2O + 2H_2O \tag{8}$$

The gradual degradation of the steel–concrete interface precipitates the genesis and propagation of rust expansion cracks. Multiple theoretical models have been proposed to elucidate rust cracking emanating from the corrosion of carbon steel rebars within concrete. These models are founded on investigations that delve into the dynamic evolution characteristics of rust expansion cracks and corrosion byproducts throughout the rusting process.

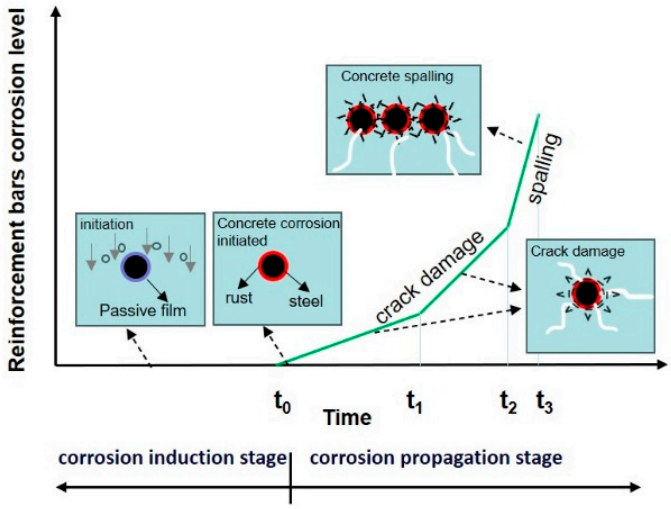

Figure 1. Full-life model of steel bar corrosion in concrete.

Initially, researchers proposed the three-stage theory of rust cracking [31], which provides a comprehensive framework for understanding the progression of rust-induced damage. This theory categorizes the rust cracking process into three distinct stages: the initial unrestricted expansion of corrosion products, the development of tensile stress within the protective concrete layer, and the eventual cracking of the concrete cover (as depicted in Figure 2a).

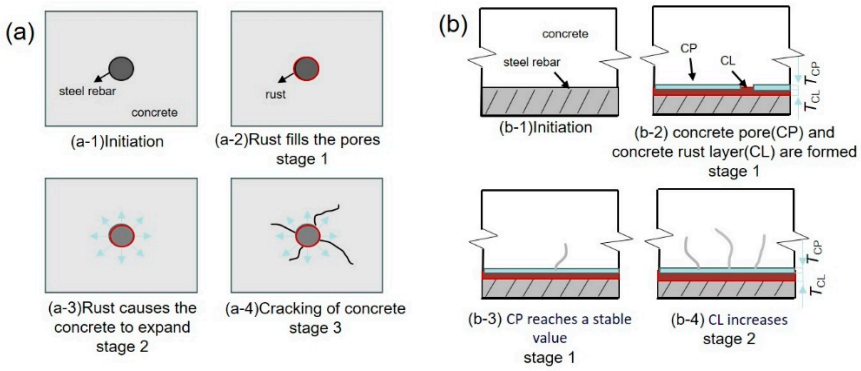

Figure 2. Schematic diagram of the three-stage theory (**a**) and two-stage theory (**b**) of concrete rust cracking.

More recently, K. Wang and Zhao Yuxi et al. proposed an alternative two-stage theory of rust cracking [32] (as shown in Figure 2b), offering a refined perspective on the rust cracking process. The first stage is characterized by the initial blunting of the steel rebar and the gradual filling of concrete pores with corrosion products until a stable equilibrium is reached. The second stage is marked by a halt in the growth of the corrosion product-filled concrete pores, while the thickness of the concrete rust layer (CL) continues to expand, ultimately leading to visible rusting and cracking at the concrete surface.

The fundamental divergence between the two rust cracking theories lies in their differing views on whether corrosion products simultaneously occupy concrete pores, accumulate at the steel–concrete interface, and infiltrate the rust expansion cracks. Understanding these dynamics is crucial for predicting and mitigating the effects of rust cracking in reinforced concrete structures.

The dynamic evolutionary traits of rust expansion cracks and corrosion products hold paramount significance in the rust cracking process, serving as vital research avenues for the establishment of reinforced concrete rust cracking models. The aforementioned theories

provide an explanation for the phenomenon of concrete rust cracking, which is attributed to the corrosion of carbon steel.

2.3. The Main Factors Affecting the Corrosion of Steel Rebars in Concrete

A range of factors, enumerated in previous studies, exert a significant influence on the corrosion process of steel bars embedded within concrete [33–35]. These factors can be broadly categorized into three principal domains: the inherent properties of the steel bars, the characteristics of the surrounding concrete, and the external environmental factors. In the subsequent discussion, we shall concentrate on two of the most prominent factors contributing to steel corrosion: chloride ion erosion and concrete carbonization.

2.3.1. Chloride Ion Erosion

Chloride ions (Cl^-) predominantly originate from environments where chloride concentrations are elevated, such as marine settings, salt lakes, saline–alkali regions, and areas affected by road deicing salts. Additionally, the use of seawater and sea sand in the preparation of concrete specimens or admixtures can introduce chlorides, facilitating the penetration of Cl^- into the steel rebars within the concrete. The rate at which chlorides diffuse is influenced by several factors, including the permeability and porosity of the concrete matrix [36].

The corrosion mechanism of Cl^- on steel rebars primarily involves the undermining of passivation films, the establishment of corrosive galvanic cells, and catalytic actions [37–41]. Cl^- ions, unlike other anions, selectively adsorb onto the surface of steel rebars, inflicting damage upon the passivation film. The accumulation of Cl^- ions on the rebar surface leads to a significant reduction in the local concentration of OH^- ions, particularly when compared to the concentrations found in concrete pore fluids, resulting in a swift decrease in pH levels. Consequently, the passivation film is more susceptible to damage, which in turn accelerates the corrosion of the exposed reinforcement.

As the corrosion progresses, it results in the formation of galvanic cells. Over time, the intensified accumulation of chloride ions on the rebar surface leads to localized corrosion [42]. This localized corrosion creates a potential difference between areas where the passivation film remains intact and the corroded steel, thus establishing galvanic cells. The ongoing penetration of Cl^- into the compromised passivation film increases the ionic conductivity between the corroded areas, diminishing the electrical resistivity [43–45].

Furthermore, Cl^- ions act as catalysts in the corrosion process. They react with Fe^{2+} to form soluble $FeCl_2$, which then reacts with OH^- in the concrete to precipitate $Fe(OH)_2$. Upon exposure to H_2O and O_2, the reaction sequence continues, resulting in the formation of $Fe(OH)_3$ and perpetuating the corrosion of the steel rebars [46].

2.3.2. Concrete Carbonization

In addition to chloride ions, carbon dioxide (CO_2) serves as a contributory factor in enhancing the likelihood of steel corrosion. CO_2 gas has the ability to permeate the interior of concrete, interacting with hydration products, altering its internal structure, and causing a notable decrease in the pH value of the concrete pore solution [22]. This phenomenon is referred to as concrete carbonization. The impact of carbonization on steel bar corrosion is primarily manifested in two principal aspects: Firstly, the decrease in concrete alkalinity has a deleterious effect on the stability and homogeneity of the passivation film that coats the steel bar surface, subsequently enhancing corrosion activity within the concrete matrix. Secondly, as the alkalinity of the concrete pore fluid diminishes, the chloride aluminate undergoes decomposition. Consequently, this process results in a continuous increase in the concentration of free chloride ions within the concrete pore fluid, thereby exacerbating the corrosion rate of the reinforcement. MA Sanjuán, et al. [47] studied the carbonation process of concrete under natural and accelerated conditions, enabling the accelerated carbonation test results to reasonably explain the carbonation process of concrete. Moreover, Xie M, et al. [48] recently proposed in their research that the durability design of reinforced concrete

structures should not only prevent the entry of chlorides, but also take into account the simultaneous occurrence of carbonation corrosion processes.

3. Corrosion Experimental Methods for Steel Rebars in Concrete

The corrosion experimental methods typically utilized for reinforced concrete specimens encompass various techniques, including the electrification-accelerated corrosion method [49], the salt spray corrosion testing approach, and the aggressive solution immersion method [50], among others. Herein, we concisely delve into several commonly employed techniques that aim to study corrosion processes.

3.1. Natural Corrosion Test Method

The natural corrosion test involves exposing reinforced concrete specimens to natural environmental conditions, ultimately resulting in the corrosion of steel reinforcement embedded within the concrete matrix. A key advantage of this testing approach is its ability to closely mimic the corrosion process of steel reinforcement observed in real-world engineering scenarios [3,20]. However, this method is fraught with drawbacks, including prolonged testing durations, significant tracking and recording workloads, cumbersome management procedures, and the neglect of the coupled effects of force and the environment [51]. Given the aforementioned limitations, the natural corrosion method is typically not employed for investigating the corrosion mechanisms of steel reinforcement, but instead serves as a comparative tool against other corrosion techniques.

3.2. Artificial Climate Simulation Method

The artificial climate simulation method is a testing procedure that replicates one or multiple factors present in atmospheric environments, encompassing CO_2 concentrations, lighting conditions, temperature fluctuations, humidity levels, and simulated rainfall, all within a controlled laboratory setting. This methodology results in a reduction of the durability of reinforced concrete specimens [33], effectively simulating the wear and tear experienced under diverse environmental conditions. Researchers replicated the combined effects of temperature variations, humidity levels, solar radiation, and simulated precipitation within a naturalistic environment [28,52]. Hailong Ye et al. used the artificial climate method to study the impact of corrosion characteristics and structural performance of loaded reinforced concrete beams, establishing a unique strong linear relationship between the average mass loss of corroded rebar and the maximum corrosion-induced crack width. Applying bending loads during the corrosion process exacerbates the corrosion in the pure flexural zone [53]. Recently, Weipeng Feng et al. conducted a systematic comparison and evaluation of the accelerated corrosion of steel reinforcement in concrete induced by chloride ions using the artificial climate environment method, and the key influencing factors that affect the corrosion results include current density, salt concentration, service load [54].

This approach effectively emulated electrochemical corrosion mechanisms akin to those encountered in natural settings, while significantly accelerating the degradation process of reinforced concrete specimens. While the artificial climate simulation method approximates the natural corrosion method, there remains a dearth of research validating the congruency of experimental outcomes between the two methodologies. Consequently, it is imperative to intensify investigations pertaining to the similarities and discrepancies between these two approaches. Additionally, the artificial climate simulation method exhibits certain limitations, including elevated experimental costs, protracted experimental cycles, and limited accuracy in predicting steel corrosion rates.

3.3. Electrification Accelerated Corrosion Method

In comparison to the previously mentioned corrosion techniques, the electrically accelerated corrosion test has emerged as a preeminent method for studying corrosion, attributed to its ease of operation, versatility, and capability to expeditiously investigate

the corrosion processes of reinforced concrete. Figure 3a shows schematic and physical diagrams of the rebar–mortar samples, and Figure 3b shows a schematic diagram of the applied constant current accelerated corrosion test [55]. The reinforced concrete specimen is connected to the positive terminal of the external power supply unit, establishing the initial electrical configuration. Meanwhile, the stainless-steel mesh is connected to the negative terminal, serving as the counter-electrode. Upon the application of electricity, electrons are emitted from the anode, triggering the onset of corrosion within the steel reinforcement. According to their operational principles, the electrically accelerated corrosion tests are generally categorized into two types: the external constant voltage accelerated corrosion test and the external constant current accelerated corrosion test. It is noteworthy that the constant current accelerated corrosion method has been extensively utilized for simulating the corrosion processes of steel reinforcement embedded in concrete within controlled laboratory environments [56,57].

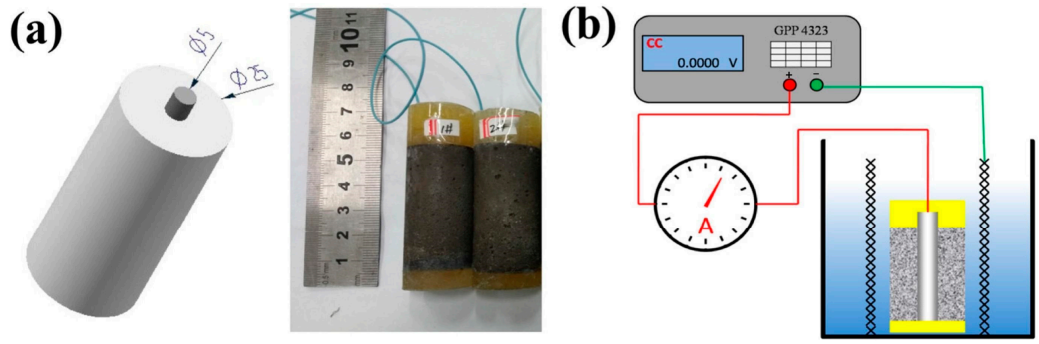

Figure 3. (**a**) Schematic diagram and photograph of rebar–mortar sample and (**b**) schematic illustration of the applied constant current accelerated corrosion test. Reprinted from Ref. [55].

Despite this, the electrically accelerated corrosion test possesses inherent limitations, necessitating further exploration into the correlation between the experimental outcomes and natural corrosion processes.

3.4. Salt Spray Corrosion Test Method

The salt spray corrosion test deliberately aims to expedite the corrosion process of steel bars within a tightly controlled environment of a salt spray chamber. Specifically, the salt spray corrosion test includes several different types, such as Neutral Salt Spray (NSS), Acidified Acid Salt Spray (AASS), and Copper Accelerated Acid Salt Spray (CASS). Among them, the Neutral Salt Spray test is one of the earliest and most widely used methods. It uses a 5% sodium chloride solution and adjusts the pH value of the solution to a neutral range (6 to 7) as the solution for spraying. This test effectively assesses the corrosion resistance of metal materials and their coatings by meticulously controlling key parameters [58,59]. The test temperature, chloride concentration, and exposure duration are all crucial factors that are meticulously manipulated to achieve this objective. M.P. Papadopoulos et.al conducted accelerated corrosion salt spray tests on new types of rebars to study their corrosion behavior and establish a correlation with naturally corroded rebars of the same grade [60].

Notably, by increasing the concentration of chloride salts, we can significantly shorten the duration necessary to inquire into the corrosion process of steel rebars. Consequently, this approach greatly enhances the efficiency of our research endeavors. Furthermore, this method exhibits a substantial correlation with natural corrosion processes, effectively replicating the corrosion mechanisms of reinforcement in environments characterized by elevated chloride concentrations.

3.5. Other Accelerated Corrosion Methods

Apart from the primary accelerated corrosion techniques previously discussed, a comprehensive array of methods is encompassed, encompassing the electrochemical corrosion experiments [55,57–59,61], internal chloride salt corrosion test [62], and the dry–wet cycle accelerated corrosion test [63]. These experiments are designed to expedite the corrosion process through controlled manipulations, including increasing the environmental temperature or humidity to enhance the rate of chemical reactions, raising the concentration of chloride ions to simulate aggressive environments, and forming galvanic cells that can accelerate the anodic dissolution of steel. Each accelerated corrosion technique possesses distinct applicability and inherent constraints. When selecting appropriate accelerated corrosion methods, it is imperative to take into account diverse factors, including cost containment, the duration of testing, and correlation, etc., to facilitate a swift yet accurate assessment of the corrosion resistance of steel bars.

4. Analysis of Corrosion Products and Interface Characteristics of Steel Rebars by X-CT Technology

In comparison to alternative observation techniques employed for examining the corrosion morphology of steel rebars embedded within concrete, X-CT technology exhibits a distinguished edge. This innovative approach eliminates the necessity for sample destruction, thus enabling a non-invasive evaluation while faithfully reproducing the corrosion patterns of steel bars and the distribution of corrosion products within the concrete matrix. Furthermore, the scope of X-CT detection is remarkably broad, encompassing not only the assessment of corrosion states in concrete-embedded steel bars, but also the quantitative analysis of pore defects within concrete structures.

4.1. X-CT Technology Principles

The underlying mechanism of CT scanning technology, as elaborated in references [64,65], involves employing X-rays to systematically scan a specific region of interest within the sample from various angles. Subsequently, data pertaining to the attenuation of the X-rays by the sample are meticulously gathered. These collected data then undergo an image reconstruction process, utilizing a specialized algorithmic framework implemented by a computer. Upon completion of this reconstruction, the detailed information pertaining to the scanned section is seamlessly presented in the format of a grayscale image. From these outputted cross-sectional images, one can effortlessly discern crucial insights into the test sample's structure, material composition, defects, and other intricate internal features.

4.2. Application of X-CT Technology in Concrete Structures

Concrete structures, inherently complex and heterogeneous, are susceptible to the development of internal cracks under the influence of applied loads. The cracks undergo a gradual process of expansion, concurrent with the acceleration of the corrosion process of the embedded steel reinforcement by deleterious substances present within the external environment. As time elapses, the corrosion products of the steel bars accumulate and expand, ultimately resulting in the disintegration of the concrete matrix and a subsequent decrement in the structural durability of the concrete element. Consequently, it is imperative to initiate an investigation at the microstructural level of concrete, encompassing the detection of cracks, the analysis of the distribution of steel corrosion products, and the assessment of any associated concrete damage.

In 1980, Morgan [66] employed medical CT scanning techniques to examine concrete specimens, successfully yielding distinct images of concrete aggregates, mortar, and cracks. Subsequently, John et al. [67] replicated these findings through meticulous experimentation. In China, research efforts on utilizing CT technology for the quantitative analysis of internal cracks in concrete are steadily escalating. Chen Houqun [68] delved into two principal challenges that had remained unresolved in prior studies: the capability of CT technology to detect cracks influenced by aggregates and its accuracy in pinpointing the

precise location of these cracks. Tian W. et al. [69] derived a three-dimensional model of the internal microstructure of concrete through meticulous analysis of CT data, thereby providing theoretical grounding for the quantitative and spatially resolved analysis of crack distribution within concrete structures.

4.3. Research on Steel Corrosion Products and Interface Characteristics Based on X-CT Technology

Extensive research has conclusively demonstrated a key contrast: while the concrete matrix remains robust, the interface between steel and concrete is disproportionately prone to deterioration [70–74]. Stemming from the interfacial phenomenon occurring between disparate materials, a myriad of defects, including pores and cracks, proliferate within this region, ultimately resulting in the localized depletion of the $Ca(OH)_2$ layer. Notably, these interfacial defects exert both salutary and deleterious effects on reinforced concrete structures.

1. The salutary aspect lies in the fact that as the corrosion of steel intensifies, a substantial quantity of corrosion products is generated on the steel matrix's surface. Under such circumstances, the interface area, enriched with pores, serves as a repository for these corrosion products, significantly mitigating the expansion stress exerted by them and extending the durability of the concrete protective layer by delaying its cracking;
2. The deleterious impact stems from the inadequate $Ca(OH)_2$ protective layer present at the interfacial defects prior to the deterioration of the steel reinforcement's passivation film. Consequently, the critical concentration of Cl^- is significantly increased in these regions compared to other parts, leading to an accelerated erosion by Cl^- and an exacerbation of the destructive effects on the passivation film.

The aforementioned effects underscore the imperative to delve deeper into the impact of interface areas on the comprehensive process of steel corrosion. Nevertheless, prior studies primarily resorted to the slicing and breaking method for observing the morphological characteristics of the reinforced concrete interface. This method would cause huge damage and destruction to the experiment itself, affect the authenticity of the experimental results, and cannot continuously observe the long-term development of the sample. Fortunately, the application of X-CT has solved the above problems, allowing for intuitive and non-destructive observation of the internal structure of concrete [75,76].

Beck et al. [77] pioneeringly employed X-CT technology to elucidate the chloride-induced corrosion process of steel rebars within concrete, ultimately revealing cracks of micrometer dimensions. By subjecting carbon steel and ferritic stainless steel to accelerated corrosion processes via the application of electrical current, Itty et al. [78] employed X-CT technology to meticulously analyze the accumulation of corrosion products, the emergence and propagation of cracks, the infiltration of corrosion products into cracks and pores, as well as their subsequent distribution, while also elucidating disparities in corrosion morphologies exhibited by the two materials. Cesen et al. [79] comprehensively assessed the corrosion risks associated with steel rebars by synergistically incorporating X-CT technology with SEM (Scanning Electron Microscopy), further deepening their understanding of the corrosion mechanisms within concrete through the integration of X-CT technology with electrochemical testing. Savija et al. [80] embarked on a comprehensive and multifaceted investigation, utilizing a diverse array of experimental techniques to delve deeply into the intricate processes underlying the cracking of concrete protective layers resulting from steel corrosion, offering unique insights from diverse perspectives, Notably, X-CT technology was utilized to meticulously monitor the progressive formation of rust during the accelerated corrosion process of steel rebars, as well as the gradual emergence and propagation of cracks within the concrete protective layers. Dong Biqin et al. [81] proposed the applicability of X-CT technology, and experimental results showed that X-CT technology can clearly obtain information on corrosion pits, corrosion products, as well as mortar cracking induced by corrosion throughout the entire sample, and they enable tracking of the temporal development of steel corrosion products, as well as monitoring the emergence and subsequent expansion of mortar cracks resulting from the accumulation of

corrosion products. Michel [82] successfully integrated X-CT technology with DIC (Digital Image Correlation) technology, thereby enabling a thorough qualitative and quantitative analysis of the data pertaining to steel corrosion products infiltrating the surrounding cement matrix. Consequently, a robust conceptual model was established, accurately depicting the infiltration process of steel corrosion products into cement-based materials. Weilin Liu et al. [55] utilized X-CT technology to thoroughly investigate the corrosion behavior exhibited by alloyed steel rebar–mortar and carbon–steel rebar–mortar specimens after conducting electromigration chloride-accelerated corrosion experiments, as shown in Figure 4. The study revealed that alloyed steel rebar exhibited a certain degree of localized corrosion, along with limited amounts of corrosion products, see Figure 4b. In contrast, the carbon–steel rebar exhibited severe general corrosion, see Figure 4a. In summary, X-CT technology plays a pivotal role in examining the distribution of steel corrosion products and elucidating the characteristics of steel/concrete interfaces within concrete structures.

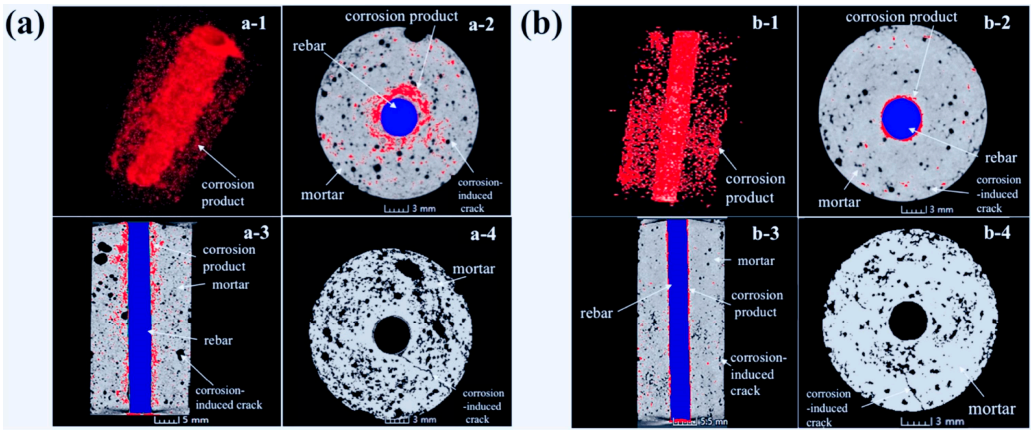

Figure 4. CT images for a (**a**) CSRM (carbon–steel rebar–mortar) sample and (**b**) ASRM (alloyed steel rebar–mortar) sample: (**a-1**,**b-1**) three-dimensional distribution of the corrosion product, (**a-2**,**b-2**) circular section, (**a-3**,**b-3**) vertical section, and (**a-4**,**b-4**) the distribution of corrosion-induced cracks. Reprinted from Ref. [55].

5. Methods for Improving the Corrosion Resistance of Steel Rebars in Concrete Structures

Prolonging the lifespan of reinforced concrete structures, extending its durability, is important not only for economic reasons but also for making the entire system more sustainable, using fewer raw materials, producing less material, and prolonging the lifespan of existing materials.

Several promising strategies have been proposed to enhance the durability of reinforced concrete structures. Firstly, our focus lies in fortifying the concrete protective layer to effectively prevent the infiltration of harmful substances into the concrete matrix. Secondly, researchers have prioritized enhancing the inherent corrosion resistance of steel rebars. As an example, the incorporation of alloy elements has been explored to develop innovative steel rebars with superior corrosion resistance. Additionally, measures to reinforce the adhesion at the interface between steel rebars and concrete are equally important. This section delves into the principal measures designed to mitigate the corrosion of reinforced concrete, thereby extending its service life.

5.1. Methods to Improve the Quality of the Concrete Protective Layer

5.1.1. Enhancing the Compactness of the Concrete Protective Layer

Industry and academic experts maintain that enhancing the compactness of concrete holds a pivotal role in mitigating steel reinforcement corrosion. A concurrent increase in compactness and decrease in porosity of concrete leads to an elevation in its apparent quality. The porosity of concrete significantly alters its physical and mechanical properties

by affecting its internal structure, such as microcracks and voids. The higher the porosity, the lower the key mechanical parameters of concrete, including elastic modulus, strength, and compressive strength, and its deformation process and failure mechanism will also differ [83]. Therefore, meticulous control over porosity is essential in the design and application of concrete, as it helps to mitigate the penetration of deleterious substances, like chloride ions (Cl^-), into the material's core. Even so, certain specific applications may require a higher porosity to meet particular performance requirements. For instance, permeable concrete needs a larger porosity to achieve high permeability, but an excessively high porosity can lead to a significant decrease in strength [83]. Moreover, when concrete is subjected to high temperatures, it is prone to spalling due to its dense structure and low permeability, which can cause a sharp reduction in load-bearing capacity [84,85].

The water–cement ratio is a key parameter that determines the strength, durability, and a host of other physical and mechanical properties of concrete. When the water–cement ratio is high, there are relatively fewer cement particles in the concrete mixture, resulting in larger distances between them [86]. The colloid produced by hydration is not sufficient to fill the gaps between particles, leading to increased porosity and a reduction in concrete strength. On the contrary, when the water–cement ratio is low, the distance between cement particles is smaller, and the colloid produced by cement hydration easily fills the gaps between particles. The amount of water pores left after evaporation is also lower, resulting in higher concrete strength [87].

The type of aggregate significantly influences the porosity of concrete. Different types of aggregates (e.g., basalt, pumice, sandstone, and limestone) exhibit varying characteristics in terms of bubble count, spacing factor, and average pore diameter within the concrete [87–89]. For instance, limestone concrete has the highest bubble count, while sandstone concrete has the fewest, directly impacting the concrete's pore structure and micro-interface features. Furthermore, the parent rock type of the aggregate affects its performance indicators such as packing porosity, crushing value, soundness, and water absorption rate, which in turn affect the overall performance of the concrete.

The size of aggregate particles also significantly affects the porosity and mechanical properties of concrete [90,91]. Larger coarse aggregates can offer higher strength and durability but may also increase the fluidity and workability of the concrete. Specifically, as the size of coarse aggregate particles increases, the compressive strength, Young's modulus, and tensile strength of concrete exhibit a trend of initially increasing and then decreasing. The presence of needle-like or flaky particles reduces the concrete's strength and workability because these particles have a large surface area that demands more cement paste to coat their surfaces.

In light of this, international organizations have formulated a comprehensive set of pertinent standards governing the construction of concrete structures intended for marine environments [76]. Typically, the primary strategies involve the selection of thicker concrete protective layers, increased cement dosages, and reduced water–cement ratios, aimed at enhancing the compactness and durability of concrete.

However, the composition of concrete is complex, and there are many factors that affect its performance, so the applicability of the experimental-based assessment method for mix design is limited. Recently, Shiqi Wang et al. proposed an intelligent multi-objective optimization algorithm program for concrete based on machine learning, which takes into account factors such as compressive strength, chloride resistance, environmental impact, and life cycle cost [92]. This program can fully evaluate the durability and environmental performance of concrete including recycled materials. In the future, with the help of intelligent algorithms of machine learning, the method for optimizing the design of concrete performance will be further improved.

5.1.2. Apply a Protective Coating to the Concrete Surface

Concrete, a complex structure composed of numerous pores, facilitates the entry of harmful substances through these pores, thereby eroding the reinforcement substrate.

Consequently, the judicious selection of protective coatings, including epoxy resin and polyvinyl acetate, can effectively barricade the ingress of exterior harmful agents. In recent years, sustainable use of bio-based coatings has become increasingly important due to the need for environmental protection. Sarcinella, A and Frigione, M summarized the research progress of environmentally friendly coatings that can be used for concrete corrosion prevention. Many biofriendly coatings were mentioned, such as oils extracted from plants and raw materials extracted from agricultural and animal waste [93,94]. Despite all this, protective coatings are not without their drawbacks. Firstly, they are cost-intensive. Furthermore, the discrepancy in shrinkage behavior between concrete and the coating can lead to the development of cracks, particularly when the curing coating is excessively thick, thereby compromising its protective effectiveness for the concrete structure. Taking into account both the notable advantages and inherent limitations, coatings applied onto the concrete surface have the potential to attenuate the corrosion rate of reinforced concrete structures, albeit within certain limitations. However, their application remains impracticable in large-scale construction projects that necessitate an extended service life cycle [95].

5.2. Methods to Improve the Corrosion Resistance of Steel Rebars

5.2.1. Apply Surface Coating of Steel Rebars

The surface coating of steel bars encompasses two distinct types: the first being non-metallic coatings [96], exemplified by epoxy resin, which possesses a dense structure. Boasting excellent performance and remarkable stability, this coating effectively mitigates the contact between external corrosive agents and the steel reinforcement matrix. Nevertheless, epoxy resin coating is not without its shortcomings. The application of epoxy resin coating on steel bar surfaces diminishes the roughness of threaded steel bars, subsequently weakening the bonding force between the steel bars and concrete. Another type is metal coatings, which are mainly composed of some active metals [97]. Among these, hot-dip galvanized steel bars are extensively utilized for steel bar surface coating due to their numerous advantages, including low cost, simplicity of process, and robust adhesion to steel bars [98]. It is lauded for its cost-effectiveness, straightforward application process, and robust adherence to the steel surface. Galvanized coatings provide a sacrificial protection mechanism, where the zinc layer corrodes preferentially, sparing the underlying steel. However, galvanized steel bars exhibit poor resistance to Cl^- corrosion, rendering them unsuitable for deployment in environments with elevated Cl^- concentrations.

The dichotomy between epoxy and galvanized coatings lies in their ideal application scenarios. Epoxy coatings, while excellent for resisting general corrosive attack, may necessitate additional measures to prevent cracking. Galvanized coatings, despite their economic and application advantages, are less effective in extreme corrosive conditions and may not be the best choice for structures with a critical need for longevity. Recognizing these limitations, the research community is actively investigating hybrid systems that can leverage the strengths of both coating types [99,100], One such innovation is the zinc/epoxy resin dual coating [101]. which combines the immediate sacrificial protection of zinc with the long-term barrier properties of epoxy. This dual coating is particularly promising for use in severe corrosion environments and is designed to endure surface abrasions and maintain the steel's corrosion resistance throughout its service life.

Moreover, ongoing research is exploring advanced coating materials, such as nanocomposite coatings [102] and environmentally friendly alternatives [103], which could offer improved durability, self-healing capabilities, or reduced environmental impact. These advancements aim to address the economic, environmental, and performance aspects of corrosion protection for reinforced concrete structures, pushing the boundaries of what is possible with current technologies.

5.2.2. Alloying Design of Steel Rebars for Corrosion Resistant

Through meticulous regulation of the proportions and types of alloying elements, alloy steel rebars are adept at fulfilling the requisite corrosion resistance and mechanical properties throughout the lifespan of reinforced concrete structures across diverse environmental conditions. The careful balance of carbon content and the addition of alloying elements like chromium, nickel, and molybdenum are critical in tailoring the rebar's properties to meet specific performance criteria [104].

Typically, the quantity of carbon present in steel rebars exhibits a direct correlation with their strength, while inversely correlating with their toughness. Therefore, reducing carbon content and incorporating additional corrosion-resistant alloy elements is of paramount importance in enhancing both the corrosion resistance and organizational uniformity of steel rebars [14]. This approach allows for the development of rebars that maintain their structural integrity while providing enhanced resistance to environmental aggressors.

Given the rigorous demands on the durability of reinforced concrete structures in highly corrosive environments, stainless steel rebars incorporating corrosion-resistant alloy elements have emerged as a viable solution [105]. Stainless steel reinforcement not only satisfies the necessary criteria for corrosion resistance but also exhibits high plasticity, strength, exceptional fatigue resistance, and high-temperature tolerance. This is attributed to the inclusion of corrosion-resistant alloy elements, such as aluminum (Al) and chromium (Cr), which facilitate the formation of a densely packed passivation film on the surface of stainless-steel reinforcement. These passivation films effectively mitigate steel corrosion, providing a protective barrier against corrosion-inducing agents.

Notably, stainless steel reinforcement maintains robust corrosion resistance, particularly in hostile environments characterized by elevated chloride (Cl^-) concentrations and concrete carbonization. However, stainless steel reinforcement is often hindered by issues such as poor weldability, elevated costs, and the potential for pitting and macrocell corrosion. Consequently, the utilization of stainless steel reinforcement is constrained due to these limitations.

Extensive research has been conducted by Hurley M F [106] and Mohamed N [107] regarding the passivation and corrosion behavior of alloy reinforcement in simulated concrete pore solutions. Their groundbreaking findings demonstrate a significant enhancement in the corrosion resistance capabilities of the reinforcement. Notably, the threshold chloride ion concentration required for de-passivation is 2–10 times higher in comparison to traditional carbon steel reinforcement. The passivation film formed on alloy reinforcement exhibits a stark contrast to that observed on carbon steel reinforcement. Remarkably, the alloy reinforcement exhibits a dual-layered passivation film, endowing it with superior corrosion resistance. Shi Jinjie et al. further delved into the intricate rust layer structure of low-alloy steel reinforcement within a simulated concrete pore solution [108]. The existence of the rust layer on alloy steel reinforcement effectively mitigates the corrosion rate of the steel reinforcement, thus enhancing its durability.

The aforementioned research comprehensively demonstrates the robust corrosion resistance characteristics exhibited by alloy steel rebars, underscoring their durability in challenging environments. Additionally, it provides preliminary yet insightful glimpses into the corrosion behavior of these rebars within simulated concrete pore solutions, paving the way for future investigations. Furthermore, the research delves into the fundamental reasons behind the enhanced corrosion resistance of these alloys, offering valuable insights into their mechanisms. While simulated concrete pore solutions offer a certain degree of reflection of the microenvironment surrounding steel rebars in concrete, the dynamic changes and uneven spatial distribution characteristics prevalent in the heterogeneous gas-solid-liquid multi-phase system of concrete remain elusive within these simulated environments. Consequently, the elucidation of the corrosion behavior and underlying mechanisms of alloy steel rebars within authentic concrete environments remains a pressing issue that demands urgent attention within this research domain.

5.2.3. Electrochemical Protection of Steel Rebars

Broadly categorized, the electrochemical protection techniques for steel rebars encompass two primary methods: the impressed current approach and the sacrificial anode technique. The sacrificial anode protection method depicted in Figure 5 involves the utilization of active metals, such as Magnesium alloy, as sacrificial anodes [109]. These anodes sacrificially undergo corrosion, effectively substituting for and mitigating the corrosion of cathodic metals, thereby precluding electrochemical degradation of the matrix. Among its advantages, the sacrificial anode method stands out for its independence from external current, cost-effectiveness, simplicity, and feasibility. This method is particularly suitable for environments containing chloride ions (Cl^-), where it exhibits robust performance. Nevertheless, the high consumption rate and limited service lifespan of active metals employed as anodes hamper their ability to provide sustained protection over extended periods. The impressed current method, as depicted in Figure 5, entails connecting inert metals, which have a lower electrochemical activity compared to the protected metals, to the positive terminal of an external electrical circuit. Simultaneously, the protected metal such as steel bar matrix is interconnected with the negative terminal, functioning as a cathode where hydroxyl ions (OH^-) are steadily produced. This mechanistic process results in a gradual elevation of the pH level in close proximity to the steel bar, thereby encouraging the development of a protective passivation film on its exterior surface [95]. Furthermore, this innovative method effectively attenuates the concentration of chloride ions in the vicinity of the steel reinforcement, exerting a significant protective effect on both the integrity and durability of the steel reinforcement system.

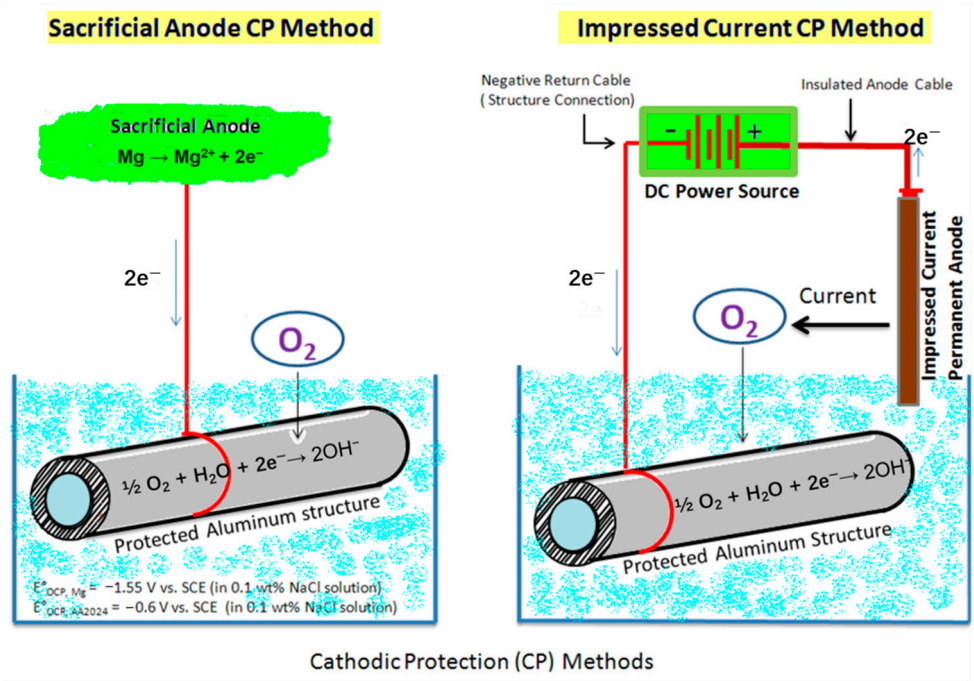

Figure 5. Electrochemical protection: Sacrificial anode method; Impressed current method. Reprinted from Ref. [109].

5.3. Methods to Strengthen the Bond between Steel Rebars and Concrete

The steel–concrete interface (SCI) is an essential element within reinforced concrete structures, as its characteristics directly influence the structural integrity and longevity. Key physical parameters at the SCI include bond strength and friction coefficient, which are critical for the mechanical interplay between steel rebars and concrete [29,110–112]. The bond's formation is characterized by the interplay of bond stress and interface slip, with chemical adhesion, rib interlocking of the deformed rebars, and frictional resistance being the primary contributors to this bond.

Measures Strengthening the bond between steel reinforcement and concrete is a multifaceted endeavor that encompasses material selection, construction techniques, and theoretical calculations [113]. The interfacial strength of concrete can be notably enhanced through advanced mixing techniques like vibration mixing or sequential batching [114]. These processes refine the concrete's internal structure, leading to improved performance. Surface roughness also plays a pivotal role in bond strength; increasing it can significantly boost friction against steel reinforcement. For example, augmenting the interfacial roughness in polyurethane concrete substantially strengthens its bond with cement concrete [115]. Innovative composite bonding technologies that integrate external bonding with mechanical anchoring, such as anchoring CFRP (Carbon Fiber Reinforced Polymer) fabrics using steel plates and bolts, effectively prevent delamination and leverage the full tensile strength of CFRP [116]. The shape and surface treatment of steel reinforcement influence bond strength as well, with ribbed reinforcement outperforming smooth due to increased mechanical interlocking from its textured surface [111]. Additionally, employing high-strength materials, such as Ultra-High Performance Concrete (UHPC), significantly amplifies concrete's mechanical properties and durability, thereby fortifying its bond with steel reinforcement. UHPC demonstrates superior interfacial shear strength and ductility compared to conventional concrete [117]. Furthermore, developing and refining theoretical models and numerical simulation methods for bond strength allows for more precise predictions and analyses of the bonding behavior between steel and concrete [118]. For instance, utilizing bilinear softening constitutive models to depict softening in cracked areas can elucidate the bond failure mechanisms [119]. Systematic testing and analysis of bond performance, including central pull-out and full-beam tests, deepen our comprehension of the bonding mechanisms and facilitate the formulation of design recommendations [111]. Integrating these measures effectively enhances the bond strength at the steel-reinforcement to concrete interface, ensuring structural safety and reliability.

6. Conclusions and Prospect

This article presents an extensive review of the passive corrosion processes undergone by steel bars within reinforced concrete structures, along with a thorough examination of the rusting mechanisms involved. The key points of this article are summarized as follows:

1. A rigorous and meticulous analysis is undertaken to pinpoint the crucial factors that underlie the corrosion of steel bars embedded within concrete;
2. It delves into the diverse methods employed for accelerated corrosion testing of steel bars within concrete, encompassing natural corrosion tests, sophisticated artificial climate simulations, electrically accelerated corrosion techniques, and rigorous salt spray corrosion tests;
3. This study provides a comprehensive overview of the current research endeavors focused on steel bar corrosion products and interface characteristics, leveraging cutting-edge X-CT technology;
4. This paper proposes strategies to improve reinforced concrete durability, emphasizing the importance of a high-quality concrete cover to shield rebars and the development of alloy-based, corrosion-resistant rebars.

Reinforced concrete, particularly in challenging marine corrosion environments, enjoys widespread usage, thereby necessitating rigorous studies and continuous efforts to enhance its durability. Future research prospects include the following, as detailed below.

Firstly, future marine engineering requires the development of steel bars with superior corrosion resistance and strength, achieved through a detailed examination and optimization of their microstructure and mechanical properties.

Secondly, in-depth research is essential for understanding the progression of electrochemical properties and the characteristics of rust formation on alloy steel rebars. Advanced analytical methods, such as X-ray computed tomography (X-CT) and machine learning algorithms, should be employed to enhance analysis and inform innovative structural designs.

Additionally, developing low-carbon emission reinforced concrete is an urgent priority, which includes the preparation of environmentally friendly concrete systems using biological raw materials, renewable materials, and recyclable materials.

Furthermore, in-situ corrosion monitoring technology for concrete is crucial for the safety and performance assessment of reinforced concrete, and it represents an excellent direction for research.

Author Contributions: Writing—original draft preparation, Q.W.; conceptualization, Q.W., Z.W., D.S. and C.L.; methodology, C.L., X.Q., H.G. and D.S.; writing—review and editing, X.Q., Z.Z., Z.W. and Q.W.; investigation, Z.W., Z.Z. and C.L.; formal analysis, Z.Z., H.G. and X.Q.; data curation, H.G., Q.W. and D.S.; resources, Z.Z., Z.W. and X.Q., supervision D.S. All authors have read and agreed to the published version of the manuscript.

Funding: This research was funded by Natural Science Foundation of China (51878246 & 52278255) and the Jiangsu Maritime Institute Science and Technology Innovation Fund (KJCX-1808).

Data Availability Statement: No new data were created or analyzed in this study. Data sharing is not applicable to this article.

Conflicts of Interest: Author Chengtao Li was employed by the company Suzhou Nuclear Power Research Institute Co., Ltd. The remaining authors declare that the research was conducted in the absence of any commercial or financial relationships that could be construed as a potential conflict of interest.

References

1. Wang, J.; Wang, Q.; Zhao, Y.; Li, P.; Ji, T.; Zou, G.; Qiao, Y.; Zhou, Z.; Wang, G.; Song, D. Research Progress of Macrocell Corrosion of Steel Rebar in Concrete. *Coatings* **2023**, *13*, 853. [CrossRef]
2. Tang, S.W.; Yao, Y.; Andrade, C.; Li, Z.J. Recent Durability Studies on Concrete Structure. *Cem. Concr. Res.* **2015**, *78*, 143–154. [CrossRef]
3. Fu, C.; Jin, N.; Ye, H.; Jin, X.; Dai, W. Corrosion Characteristics of a 4-Year Naturally Corroded Reinforced Concrete Beam with Load-Induced Transverse Cracks. *Corros. Sci.* **2017**, *117*, 11–23. [CrossRef]
4. Cui, Z.; Alipour, A. Concrete Cover Cracking and Service Life Prediction of Reinforced Concrete Structures in Corrosive Environments. *Constr. Build. Mater.* **2018**, *159*, 652–671. [CrossRef]
5. Greve-Dierfeld, S.v.; Bisschop, J.; Schiegg, Y. Nichtrostende Bewehrungsstähle zur Verlängerung der korrosionsfreien Lebensdauer von Stahlbetonbauwerken. *Beton Stahlbetonbau* **2017**, *112*, 601–610. [CrossRef]
6. Gong, W.; Yu, H.; Ma, H.; Zhu, H. A Comprehensive Assessment of Durability and Service Life Prediction of Concrete Structures in the Simulated Tidal Zone of the South China Sea Considering Measures to Enhance Concrete Durability. *J. Build. Eng.* **2023**, *76*, 107194. [CrossRef]
7. Yu, H.; Da, B.; Ma, H.; Zhu, H.; Yu, Q.; Ye, H.; Jing, X. Durability of Concrete Structures in Tropical Atoll Environment. *Ocean Eng.* **2017**, *135*, 1–10. [CrossRef]
8. Da, B.; Yu, H.; Ma, H.; Zhang, Y.; Zhu, H.; Yu, Q.; Ye, H.; Jing, X. Investigation of durability of ordinary concrete structures in the South China Sea. *J. Harbin Eng. Univ.* **2016**, *37*, 1034–1040. [CrossRef]
9. Chen, M.; Wei, Y.; Zheng, H.; Yu, L.; Liu, Q.; Wang, Y.; Yuan, H.; Wang, C.; Li, W. Ca-LDH-Modified Cementitious Coating to Enhance Corrosion Resistance of Steel Bars. *J. Build. Eng.* **2022**, *51*, 104301. [CrossRef]
10. Shang, B.; Ma, Y.; Meng, M.; Li, Y. Feasibility of Utilizing 2304 Duplex Stainless Steel Rebar in Seawater Concrete: Passivation and Corrosion Behavior of Steel Rebar in Simulated Concrete Environments. *Mater. Corros.* **2019**, *70*, 1657–1666. [CrossRef]
11. Wang, N.; Yu, H.; Bi, W.; Zhu, H.; Gong, W.; Diao, Y. Effects of Coral Sand Powder and Corrosion Inhibitors on Reinforcement Corrosion in Coral Aggregate Seawater Concrete in a Marine Environment. *Struct. Concr.* **2021**, *22*, 2650–2664. [CrossRef]
12. Yang, L.; Liu, G.; Gao, D.; Zhang, C. Experimental Study on Water Absorption of Unsaturated Concrete: W/c Ratio, Coarse Aggregate and Saturation Degree. *Constr. Build. Mater.* **2021**, *272*, 121945. [CrossRef]
13. Li, Y.; Aoude, H. Effects of Stainless Steel Reinforcement and Fibers on the Flexural Behaviour of High-Strength Concrete Beams Subjected to Static and Blast Loading. *Eng. Struct.* **2023**, *291*, 116398. [CrossRef]
14. Rabi, M.; Shamass, R.; Cashell, K.A. Structural Performance of Stainless Steel Reinforced Concrete Members: A Review. *Constr. Build. Mater.* **2022**, *325*, 126673. [CrossRef]
15. Nie, R.; Huang, Y.; Li, X.; Sun, H.; Li, D.; Ying, J. Bond of Epoxy-Coated Reinforcement to Seawater Coral Aggregate Concrete. *Ocean Eng.* **2020**, *208*, 107350. [CrossRef]
16. Vijayaraghavan, J.; Jeevakkumar, R.; Venkatesan, G.; Rengasamy, M.; Thivya, J. Influence of Kaolin and Dolomite as Filler on Bond Strength of Polyurethane Coated Reinforcement Concrete. *Constr. Build. Mater.* **2022**, *325*, 126675. [CrossRef]
17. Wu, H.; Wang, L.; Zhang, S.; Wu, C.L.; Zhang, C.H.; Sun, X.Y. Corrosion and Cavitation Erosion Behaviors of Laser Clad FeNiCoCr High-Entropy Alloy Coatings with Different Types of TiC Reinforcement. *Surf. Coat. Technol.* **2023**, *471*, 129910. [CrossRef]

18. Wright, J.W.; Pantelides, C.P. Axial Compression Capacity of Concrete Columns Reinforced with Corrosion-Resistant Hybrid Reinforcement. *Constr. Build. Mater.* **2021**, *302*, 124209. [CrossRef]
19. Zou, G.; Wang, Q.; Wang, G.; Liu, W.; Zhang, S.; Ai, Z.; Chen, H.; Ma, H.; Song, D. Revealing Excellent Passivation Performance of a Novel Cr-Alloyed Steel Rebar in Carbonized Concrete Environment. *J. Mater. Res. Technol.* **2023**, *23*, 1848–1861. [CrossRef]
20. Dong, B.; Liu, W.; Zhang, T.; Chen, L.; Fan, Y.; Zhao, Y.; Yang, W.; Banthukul, W. Corrosion Failure Analysis of Low Alloy Steel and Carbon Steel Rebar in Tropical Marine Atmospheric Environment: Outdoor Exposure and Indoor Test. *Eng. Fail. Anal.* **2021**, *129*, 105720. [CrossRef]
21. Zhang, Z. Influence of Threshold Chloride Concentration on Corrosion Behavior of Low-Alloy Steel Rebar in Concrete Pore Solutions. *Int. J. Electrochem. Sci.* **2020**, *15*, 9864–9873. [CrossRef]
22. Liu, M.; Cheng, X.; Li, X.; Zhou, C.; Tan, H. Effect of Carbonation on the Electrochemical Behavior of Corrosion Resistance Low Alloy Steel Rebars in Cement Extract Solution. *Constr. Build. Mater.* **2017**, *130*, 193–201. [CrossRef]
23. Yoon, H.N.; Seo, J.; Kim, S.; Lee, H.K.; Park, S. Hydration of Calcium Sulfoaluminate Cement Blended with Blast-Furnace Slag. *Constr. Build. Mater.* **2021**, *268*, 121214. [CrossRef]
24. He, Y.; Mao, R.; Lü, L.; Hu, S. Hydration Products of Cement-Silica Fume-Quartz Powder Mixture under Different Curing Regimes. *J. Wuhan Univ. Technol. Mat. Sci. Edit.* **2017**, *32*, 598–602. [CrossRef]
25. Shang, B.; Ma, Y.; Meng, M.; Li, Y. Characterisation of Passive Film on HRB400 Steel Rebar in Curing Stage of Concrete. *Chin. J. Mater. Res.* **2019**, *33*, 659–665. [CrossRef]
26. Zhu, M.; Zhang, Q.; Yuan, Y.F.; Guo, S.Y.; Pan, J. Passivation Behavior of 2507 Super Duplex Stainless Steel in Simulated Concrete Pore Solution. *J. Mater. Eng Perform* **2020**, *29*, 3141–3151. [CrossRef]
27. Montemor, M.F.; Simões, A.M.P.; Ferreira, M.G.S. Chloride-Induced Corrosion on Reinforcing Steel: From the Fundamentals to the Monitoring Techniques. *Cem. Concr. Compos.* **2003**, *25*, 491–502. [CrossRef]
28. Ahmad, S. Reinforcement Corrosion in Concrete Structures, Its Monitoring and Service Life Prediction—A Review. *Cem. Concr. Compos.* **2003**, *25*, 459–471. [CrossRef]
29. Angst, U.M.; Geiker, M.R.; Michel, A.; Gehlen, C.; Wong, H.; Isgor, O.B.; Elsener, B.; Hansson, C.M.; François, R.; Hornbostel, K.; et al. The steel-concrete interface. *Mater. Struct.* **2017**, *50*, 143. [CrossRef]
30. Qiao, Y.; Wang, X.; Yang, L.; Wang, X.; Chen, J.; Wang, Z.; Zhou, H.; Zou, J.; Wang, F. Effect of Aging Treatment on Microstructure and Corrosion Behavior of a Fe-18Cr-15Mn-0.66N Stainless Steel. *J. Mater. Sci. Technol.* **2022**, *107*, 197–206. [CrossRef]
31. Liu, Y.; Weyers, R.E. Modeling the Time-to-Corrosion Cracking in Chloride Contaminated Reinforced Concrete Structures. *Materials* **1998**, *95*, 675–681. [CrossRef]
32. Wang, K.; Zhao, Y.X.; Xia, J. Experimental study and numerical simulation of corrosion-induced crack patterns of concrete structures. *J. Build. Struct.* **2019**, *40*, 138–145. [CrossRef]
33. Zhao, L.; Wang, J.; Gao, P.; Yuan, Y. Experimental Study on the Corrosion Characteristics of Steel Bars in Concrete Considering the Effects of Multiple Factors. *Case Stud. Constr. Mater.* **2024**, *20*, e02706. [CrossRef]
34. Li, H.; Yang, Y.; Wang, X.; Tang, H. Effects of the Position and Chloride-Induced Corrosion of Strand on Bonding Behavior between the Steel Strand and Concrete. *Structures* **2023**, *58*, 105500. [CrossRef]
35. Xiao, S.-H.; Cai, Y.-J.; Xie, Z.-H.; Guo, Y.-C.; Zheng, Y.; Lin, J.-X. Bond Durability between Steel-FRP Composite Bars and Concrete under Seawater Corrosion Environments. *Constr. Build. Mater.* **2024**, *419*, 135456. [CrossRef]
36. Liu, C.; Lv, Z.; Xiao, J.; Xu, X.; Nong, X.; Liu, H. On the Mechanism of Cl^- Diffusion Transport in Self-Healing Concrete Based on Recycled Coarse Aggregates as Microbial Carriers. *Cem. Concr. Compos.* **2021**, *124*, 104232. [CrossRef]
37. Han, P.; Qiao, G.; Ou, J. Corrosion Kinetic Characteristics of Carbon Steel in Thermodynamically Determined Simulated Concrete Pore Solutions Driven by the Coupling Action of Cl^- and CO_2, as Well as Alternating Polarization. *Constr. Build. Mater.* **2023**, *398*, 132506. [CrossRef]
38. Pan, D.; Niu, D.; Li, Z. Corrosion Products of Low-Alloy Steel Bars and Their Induction of Cracking in Seawater Sea-Sand Concrete Cover. *Constr. Build. Mater.* **2023**, *389*, 131800. [CrossRef]
39. Wang, Y.; Liu, Z.; Wang, Y.; Wang, D.; Yuan, C.; Liu, R. Effect of Recycled Aggregate and Supplementary Cementitious Material on the Chloride Threshold for Steel Bar Corrosion in Concrete. *Constr. Build. Mater.* **2022**, *346*, 128418. [CrossRef]
40. Gong, K.; Yang, M.; Liu, C.; Shen, X.; Xiao, L.; Li, M.; Mao, F. Synergistic Effect of Chloride Ions and Surface Film on Depassivation Mechanism of Q355B Steel in Simulated Concrete Pore Solution. *J. Build. Eng.* **2023**, *78*, 107742. [CrossRef]
41. Ji, H.; Tian, Y.; Fu, C.; Ye, H. Transfer Learning Enables Prediction of Steel Corrosion in Concrete under Natural Environments. *Cem. Concr. Compos.* **2024**, *148*, 105488. [CrossRef]
42. Long, H.; Chen, L.; Dong, B.; Sun, Y.; Yan, Y.; Chen, C. The Electronic Properties and Surface Chemistry of Passive Film on Reinforcement: Effect of Composition of Simulated Concrete Pore Solution. *Constr. Build. Mater.* **2022**, *360*, 129567. [CrossRef]
43. Ogunsanya, I.G.; Hansson, C.M. Influence of Chloride and Sulphate Anions on the Electronic and Electrochemical Properties of Passive Films Formed on Steel Reinforcing Bars. *Materialia* **2019**, *8*, 100491. [CrossRef]
44. Saremi, M.; Mahallati, E. A Study on Chloride-Induced Depassivation of Mild Steel in Simulated Concrete Pore Solution. *Cem. Concr. Res.* **2002**, *32*, 1915–1921. [CrossRef]
45. Martin, F.J.; Olek, J. Experimental Procedure for Fundamental Studies of Reinforcing Steel Corrosion Processes. *Rev. Sci. Instrum.* **2003**, *74*, 2512–2516. [CrossRef]

46. Shi, J.; Li, M.; Wu, M.; Ming, J. Role of Red Mud in Natural Passivation and Chloride-Induced Depassivation of Reinforcing Steels in Alkaline Concrete Pore Solutions. *Corros. Sci.* **2021**, *190*, 109669. [CrossRef]
47. Sanjuán, M.A.; Andrade, C.; Cheyrezy, M. Concrete carbonation tests in natural and accelerated conditions. *Adv. Cem. Res.* **2003**, *15*, 171–180. [CrossRef]
48. Xie, M.; Dangla, P.; Li, K. Reactive transport modelling of concurrent chloride ingress and carbonation in concrete. *Mater. Struct.* **2021**, *54*, 177. [CrossRef]
49. Al-Sulaimani, G.J.; Kaleemullah, M.; Basunbul, I.A.; Rasheeduzzafar. Influence of Corrosion and Cracking on Bond Behavior and Strength of Reinforced Concrete Members. *ACI Struct. J.* **1990**, *87*, 220–231.
50. Okada, K.; KobayashiI, K.; Miyagawa, T. Influence of Longitudinal Cracking Due to Reinforcement Corrosion on Characteristics of Reinforced Concrete Members. *Struct. J.* **1988**, *85*, 134–140. [CrossRef]
51. Song, Z.; Zhang, Y.; Liu, L.; Pu, Q.; Jiang, L.; Chu, H.; Luo, Y.; Liu, Q.; Cai, H. Use of XPS for Quantitative Evaluation of Tensile-Stress-Induced Degradation of Passive Film on Carbon Steel in Simulated Concrete Pore Solution. *Constr. Build. Mater.* **2021**, *274*, 121779. [CrossRef]
52. Jiang, J.; Yuan, Y. Relationship of Moisture Content with Temperature and Relative Humidity in Concrete. *Mag. Concr. Res.* **2013**, *65*, 685–692. [CrossRef]
53. Ye, H.; Fu, C.; Jin, N.; Jin, X. Performance of reinforced concrete beams corroded under sustained service loads: A comparative study of two accelerated corrosion techniques. *Constr. Build. Mater.* **2018**, *162*, 286–297. [CrossRef]
54. Feng, W.; Tarakbay, A.; Memon, S.A.; Tang, W.; Cui, H. Methods of accelerating chloride-induced corrosion in steel-reinforced concrete: A comparative review. *Constr. Build. Mater.* **2021**, *289*, 123165. [CrossRef]
55. Liu, W.; Wang, Q.; Hao, J.; Zou, G.; Zhang, P.; Wang, G.; Ai, Z.; Chen, H.; Ma, H.; Song, D. Corrosion Resistance and Corrosion Interface Characteristics of Cr-Alloyed Rebar Based on Accelerated Corrosion Testing with Impressed Current. *J. Mater. Res. Technol.* **2023**, *22*, 2996–3009. [CrossRef]
56. Ramírez-Arreola, D.; de Guadalajara, U.; Aranda-García, F.; Sedano-De-La-Rosa, C.; Camacho-Vidrio, A.; Silva, R. Corrosion behavior of steel reinforcement bars embedded in concrete with sugar cane bagasse ash. *Rev. Mex. De Ing. Quim.* **2020**, *19*, 469–481. [CrossRef]
57. Raupach, M. Corrosion of Steel Reinforcement in Concrete. *Mater. Corros.* **2009**, *60*, 77. [CrossRef]
58. Okeniyi, J.; Loto, C.; Popoola, P. Effects of *Phyllanthus muellerianus* Leaf-Extract on Steel-Reinforcement Corrosion in 3.5% NaCl-Immersed Concrete. *Met. Open Access Metall. J.* **2016**, *6*, 255. [CrossRef]
59. Okeniyi, J.O.; Loto, C.A.; Popoola, A.P.I. Corrosion Inhibition of Concrete Steel-Reinforcement in Saline/Marine Simulating-Environment by *Rhizophora mangle* L. *Solid State Phenom.* **2015**, *227*, 185–189. [CrossRef]
60. Papadopoulos, M.P.; Apostolopoulos, C.A.; Zervaki, A.D.; Haidemenopoulos, G.N. Corrosion of exposed rebars, associated mechanical degradation and correlation with accelerated corrosion tests. *Constr. Build. Mater.* **2011**, *25*, 3367–3374. [CrossRef]
61. Nie, S.-J.; Yi, X.-N.; Zhou, H.-L.; Zhu, H.-J.; Yang, L.-L.; Fu, F.-L.; Li, J.-Y.; Yang, H.-K.; Xu, G.-X.; Lu, S.; et al. Corrosion behavior of as-cast $Al_{0.75}CoFeCr_{1.25}Ni$ high entropy alloy in 0.5 mol/L NaOH solution. *Iron Steel Res. Int.* **2024**, *37*, 175–223. [CrossRef]
62. Ren, Q.; Jin, H.; Xiao, S.; Wang, F.; Chen, B. Review on long-term performance of reinforced concrete structures under simulated acid rain erosion environments. *J. Traffic Transp. Eng.* **2022**, *22*, 41–47. [CrossRef]
63. Zhao, G.; Ma, Y.; Li, Y.; Liang, J.; Wang, K.; Zhou, F. An experimental study on the effect of marine corrosion on frictional properties of sliding pairs of offshore isolated bridges. In Proceedings of the 2018 7th International Conference on Energy and Environmental Protection (ICEEP 2018), Shenzhen, China, 14–15 July 2018. [CrossRef]
64. Zhang, C.; Wang, H.; You, Z.; Yang, X. Compaction Characteristics of Asphalt Mixture with Different Gradation Type through Superpave Gyratory Compaction and X-ray CT Scanning. *Constr. Build. Mater.* **2016**, *129*, 243–255. [CrossRef]
65. Chen, X.; Ren, D.; Xu, J.; Tian, G.; Jiang, S.; Huang, M.; Zhang, A.A.; Ai, C. Investigation on Mesoscopic Pore Characteristics in Asphalt Mixtures under the Coupling Effects of Segregation-Dynamic Pore Water-Salt Corrosion Based on CT Scanning Technology. *Constr. Build. Mater.* **2023**, *404*, 133041. [CrossRef]
66. Morgan, I.L.; Ellinger, H.; Klinksiek, R.; Thomson, J.N. Examination of Concrete by Computerized Tomography. *J. Am. Concr. Inst.* **1980**, *77*, 23–27.
67. Lawler, J.S.; Keane, D.T.; Shah, S.P. Measuring three-dimensional damage in concrete under compression. *ACI Mater. J.* **2001**, *98*, 465–475. [CrossRef]
68. Houqun, C.; Shengxin, W.; Faning, D. Chapter 14—Testing Research on Large Dam Concrete Dynamic-Static Damage and Failure Based on CT Technology. In *Seismic Safety of High Arch Dams*; Academic Press: Oxford, UK, 2016; pp. 395–489. ISBN 978-0-12-803628-0.
69. Tian, W.; Han, N. Evaluation of Meso-damage Processes in Concrete by X-ray CT Scanning Techniques under Real-Time Uniaxial Compression Testing. *J. Nondestruct. Eval.* **2019**, *38*, 44. [CrossRef]
70. Glass, G.K.; Yang, R.; Dickhaus, T.; Buenfeld, N.R. Backscattered Electron Imaging of the Steel–Concrete Interface. *Corros. Sci.* **2001**, *43*, 605–610. [CrossRef]
71. Page, C.L. Initiation of Chloride-induced Corrosion of Steel in Concrete: Role of the Interfacial Zone. *Mater. Corros.* **2009**, *60*, 586–592. [CrossRef]
72. Mohammed, T.; Otsuki, N.; Hamada, H.; Yamaji, T. Chloride-Induced Corrosion of Steel Bars in Concrete with the Presence of Gap at the Steel-concrete Interface. *ACI Mater. J.* **2002**, *99*, 149–156.

73. Zhang, R.; Castel, A.; François, R. The Corrosion Pattern of Reinforcement and Its Influence on Serviceability of Reinforced Concrete Members in Chloride Environment. *Cem. Concr. Res.* **2009**, *39*, 1077–1086. [CrossRef]
74. Angst, U.M.; Elsener, B.; Larsen, C.K.; Vennesland, Ø. Chloride Induced Reinforcement Corrosion: Electrochemical Monitoring of Initiation Stage and Chloride Threshold Values. *Corros. Sci.* **2011**, *53*, 1451–1464. [CrossRef]
75. Wong, H.S.; Zhao, Y.X.; Karimi, A.R.; Buenfeld, N.R.; Jin, W.L. On the Penetration of Corrosion Products from Reinforcing Steel into Concrete Due to Chloride-Induced Corrosion. *Corros. Sci.* **2010**, *52*, 2469–2480. [CrossRef]
76. Chernin, L.; Val, D.V. Prediction of Corrosion-Induced Cover Cracking in Reinforced Concrete Structures. *Constr. Build. Mater.* **2011**, *25*, 1854–1869. [CrossRef]
77. Beck, M.; Goebbels, J.; Burkert, A. Application of X-ray Tomography for the Verification of Corrosion Processes in Chloride Contaminated Mortar. *Mater. Corros.* **2007**, *58*, 207–210. [CrossRef]
78. Itty, P.-A.; Serdar, M.; Meral, C.; Parkinson, D.; MacDowell, A.A.; Bjegović, D.; Monteiro, P.J.M. In Situ 3D Monitoring of Corrosion on Carbon Steel and Ferritic Stainless Steel Embedded in Cement Paste. *Corros. Sci.* **2014**, *83*, 409–418. [CrossRef]
79. Česen, A.; Kosec, T.; Legat, A. Characterization of Steel Corrosion in Mortar by Various Electrochemical and Physical Techniques. *Corros. Sci.* **2013**, *75*, 47–57. [CrossRef]
80. Šavija, B.; Luković, M.; Hosseini, S.A.S.; Pacheco, J.; Schlangen, E. Corrosion Induced Cover Cracking Studied by X-ray Computed Tomography, Nanoindentation, and Energy Dispersive X-ray Spectrometry (EDS). *Mater. Struct.* **2015**, *48*, 2043–2062. [CrossRef]
81. Dong, B.; Fang, G.; Liu, Y.; Dong, P.; Zhang, J.; Xing, F.; Hong, S. Monitoring Reinforcement Corrosion and Corrosion-Induced Cracking by X-ray Microcomputed Tomography Method. *Cem. Concr. Res.* **2017**, *100*, 311–321. [CrossRef]
82. Michel, A.; Pease, B.J.; Peterová, A.; Geiker, M.R.; Stang, H.; Thybo, A.E.A. Penetration of Corrosion Products and Corrosion-Induced Cracking in Reinforced Cementitious Materials: Experimental Investigations and Numerical Simulations. *Cem. Concr. Compos.* **2014**, *47*, 75–86. [CrossRef]
83. Li, L.G.; Feng, J.-J.; Zhu, J.; Chu, S.-H.; Kwan, A.K.H. Pervious concrete: Effects of porosity on permeability and strength. *Mag. Concr. Res.* **2021**, *73*, 69–79. [CrossRef]
84. Khoury, G.A. Effect of fire on concrete and concrete structures. *Prog. Struct. Eng. Mater.* **2000**, *2*, 429–447. [CrossRef]
85. Mohammed, H.; Ahmed, H.; Kurda, R.; Alyousef, R.; Deifalla, A.F. Heat-Induced Spalling of Concrete: A Review of the Influencing Factors and Their Importance to the Phenomenon. *Materials* **2022**, *15*, 1693. [CrossRef]
86. Bian, P.; Zhang, M.; Yu, Q.; Zhan, B.; Gao, P.; Guo, B.; Chen, Y. Prediction model of compressive strength of foamed concrete considering pore size distribution. *Constr. Build. Mater.* **2023**, *409*, 133705. [CrossRef]
87. Wang, X.; Li, D.; Bai, R.; Liu, S.; Yan, C.; Zhang, J. Evolution of the pore structure of pumice aggregate concrete and the effect on compressive strength. *Rev. Adv. Mater. Sci.* **2023**, *62*, 20230112. [CrossRef]
88. Aquino, C.; Inoue, M.; Miura, H.; Mizuta, M.; Okamoto, T. The effects of limestone aggregate on concrete properties. *Constr. Build. Mater.* **2010**, *24*, 2363–2368. [CrossRef]
89. Shi, Y.; Yang, H.; Chen, X.; Li, X.; Zhou, S. Influence of aggregate variety on pore structure and microscopic interface of concrete. *J. Build. Mater.* **2015**, *18*, 133–138. [CrossRef]
90. Vishalakshi, K.; Revathi, V.; Reddy, S.S. Effect of type of coarse aggregate on the strength properties and fracture energy of normal and high strength concrete. *Eng. Fract. Mech.* **2018**, *194*, 52–60. [CrossRef]
91. Ichino, H.; Kuwahara, N.; Beppu, M.; Williamson, E.B.; Himi, A. Effects of the shape, size, and surface roughness of glass coarse aggregate on the mechanical properties of two-stage concrete. *Constr. Build. Mater.* **2024**, *411*, 134296. [CrossRef]
92. Wang, S.; Xia, P.; Gong, F.; Zeng, Q.; Chen, K.; Zhao, Y. Multi objective optimization of recycled aggregate concrete based on explainable machine learning. *J. Clean. Prod.* **2024**, *445*, 141045. [CrossRef]
93. Sarcinella, A.; Frigione, M. Sustainable and Bio-Based Coatings as Actual or Potential Treatments to Protect and Preserve Concrete. *Coatings* **2023**, *13*, 44. [CrossRef]
94. Adeboye, S.; Adebowale, A.; Siyanbola, T.; Ajanaku, K. Coatings and the environment: A review of problems, progress and prospects. *IOP Conf. Ser. Earth Environ. Sci.* **2023**, *1197*, 012012. [CrossRef]
95. Pan, X.; Shi, Z.; Shi, C.; Ling, T.-C.; Li, N. A Review on Concrete Surface Treatment Part I: Types and Mechanisms. *Constr. Build. Mater.* **2017**, *132*, 578–590. [CrossRef]
96. Mao, Y.-Z.; Wei, Y.-H.; Zhao, H.-T.; Lv, C.-X.; Cao, H.-J.; Li, J. Corrosion Behavior of Epoxy-Coated Rebar with Pinhole Defect in Seawater Concrete. *Acta Metall. Sin.* **2018**, *31*, 1171–1182. [CrossRef]
97. Al-Negheimish, A.; Hussain, R.R.; Alhozaimy, A.; Singh, D. Corrosion performance of hot-dip galvanized zinc-aluminum coated steel rebars in comparison to the conventional pure zinc coated rebars in concrete environment. *Constr. Build. Mater.* **2021**, *274*, 121921. [CrossRef]
98. Maldonado, L.; Pech-Canul, M.; Alhassan, S. Corrosion of zinc-coated reinforcing bars in tropical humid marine environments. *Anti-Corros. Methods Mater.* **2006**, *53*, 357–361. [CrossRef]
99. Figueira, R.B.; Silva, C.J.R.; Pereira, E.V. Ureasilicate Hybrid Coatings for Corrosion Protection of Galvanized Steel in Chloride-Contaminated Simulated Concrete Pore Solution. *J. Electrochem. Soc.* **2015**, *162*, C666. [CrossRef]
100. Singh, D.; Ghosh, R. Molybdenum–phosphorus compounds based passivator to control corrosion of hot dip galvanized coated rebars exposed in simulated concrete pore solution. *Surf. Coat. Technol.* **2008**, *202*, 4687–4701. [CrossRef]
101. Lau, K.; Sagüés, A.A. Corrosion of Epoxy- and Polymer/Zinc-Coated Rebar in Simulated Concrete Pore Solution. *Corrosion* **2009**, *65*, 681–694. [CrossRef]

102. Wang, X.; Cao, Q.; Tang, F.; Pan, H.; Chen, X.; Lin, Z. Mechanical Properties and Corrosion Behavior of Dual-Filler-Epoxy-Coated Steel Rebar under a Corrosive Environment. *Coatings* **2023**, *13*, 604. [CrossRef]
103. Thomas, D.; Reshmy, R.; Eapen, P.; Sindhu, R.; Ulaeto, S.B.; Pugazhendhi, A.; Awasthi, M.K. Developments in smart organic coatings for anticorrosion applications: A review. *Biomass Conv. Bioref.* **2022**, *12*, 4683–4699. [CrossRef]
104. Zhang, J.; Zuo, L.; Jiang, J.; Ma, H.; Song, D. Microstructure and Properties of Seawater Corrosion Resistant Rebar Steel 00Cr10MoV. *J. Chin. Soc. Corros. Prot.* **2016**, *36*, 363–369. [CrossRef]
105. Araujo, L.A.A.; Arcilla, I.H.; Ramos, N.R.R.; Martín, J.E.T.M.; Chinchón-Payá, S.C.-P.; Montero, J.S.M.; Raggiotti, B.B.R.; Matres, V.M. Corrosion Initiation Period for Stainless Steel Reinforcement in Concrete Structures. In Proceedings of the XVI International Conference on Durability of Building Materials and Components, Beijing, China, 10–13 October 2023. [CrossRef]
106. Hurley, M.F.; Scully, J.R. Threshold Chloride Concentrations of Selected Corrosion-Resistant Rebar Materials Compared to Carbon Steel. *Corrosion* **2006**, *62*, 892–904. [CrossRef]
107. Mohamed, N.; Boulfiza, M.; Evitts, R. Corrosion of Carbon Steel and Corrosion-Resistant Rebars in Concrete Structures under Chloride Ion Attack. *J. Mater. Eng. Perform.* **2013**, *22*, 787–795. [CrossRef]
108. Shi, J.; Sun, W.; Jiang, J.; Zhang, Y. Influence of Chloride Concentration and Pre-Passivation on the Pitting Corrosion Resistance of Low-Alloy Reinforcing Steel in Simulated Concrete Pore Solution. *Constr. Build. Mater.* **2016**, *111*, 805–813. [CrossRef]
109. Pathak, S.S.; Mendon, S.K.; Blanton, M.D.; Rawlins, J.W. Magnesium-Based Sacrificial Anode Cathodic Protection Coatings (Mg-Rich Primers) for Aluminum Alloys. *Metals* **2012**, *2*, 353–376. [CrossRef]
110. Chiriatti, L.; Mercado-Mendoza, H.; Apedo, K.L.; Fond, C.; Feugeas, F. A study of bond between steel rebar and concrete under a friction-based approach. *Cem. Concr. Res.* **2019**, *120*, 132–141. [CrossRef]
111. Hachem, Y.; Ezzedine El Dandachy, M.; Khatib, J.M. Physical, Mechanical and Transfer Properties at the Steel-Concrete Interface: A Review. *Buildings* **2023**, *13*, 886. [CrossRef]
112. Chen, Q.; Zhang, J.; Wang, Z.; Zhao, T.; Wang, Z. A review of the interfacial transition zones in concrete: Identification, physical characteristics, and mechanical properties. *Eng. Fract. Mech.* **2024**, *300*, 109979. [CrossRef]
113. Zheng, X.; Yang, S.; Sun, S. Determination of the Corrosion Rate of Steel Bars in Concrete Based on the Porosity of Interfacial Zone. *Front. Mater.* **2020**, *7*, 573193. [CrossRef]
114. Li, N.; Ma, B.; Wang, Y.; Si, W.; Qin, F. Influence analyses of mixing approaches on properties of conventional and interlocking-dense concrete. *Constr. Build. Mater.* **2016**, *122*, 465–472. [CrossRef]
115. Wang, Y.; Sun, Q.; Ding, H.; Leng, S.; Cui, H.; Xu, B.; Cui, H. Investigation of Interfacial Bonding Properties of Polyurethane Concrete and Cement Concrete/Steel Reinforcement. *Adv. Mater. Sci. Eng.* **2022**, *2022*, 5644468. [CrossRef]
116. Kumar, K.; Das, S.; Garg, R.; Goyat, M.S. A Comprehensive Review on Enhancing the Strength of CFRPs through Nano-reinforcements: Applications, Characterization, and Challenges. *J. Fail. Anal. Preven.* **2024**. [CrossRef]
117. Bahmani, H.; Mostofinejad, D. Microstructure of ultra-high-performance concrete (UHPC)—A review study. *J. Build. Eng.* **2022**, *50*, 104118. [CrossRef]
118. Zhang, X.; Akber, M.Z.; Zheng, W. Prediction of seven-day compressive strength of field concrete. *Constr. Build. Mater.* **2021**, *305*, 124604. [CrossRef]
119. Han, X.-Y.; Wu, Z.-M.; Jia, M.-D.; Zheng, J.-J.; Yu, R.C. A new method for determining the tension-softening curve of concrete. *Theor. Appl. Fract. Mech.* **2023**, *126*, 103992. [CrossRef]